WOMERSLEY NUMBER EFFECT ON THE BLOOD FLOW THROUGH A STENOSED ARTERY USING THE CASSON MODEL

Cláudia Regina de Andrade
Edson Luiz Zaparoli
claudia@ita.br
zaparoli@ita.br
Instituto Tecnológico de Aeronáutica
Pça Marechal Eduardo Gomes, 50 - 12228-900 - São José dos Campos, SP, Brasil

Abstract. This work focuses on the numerical simulation of the pulsatile blood flow in a human artery, varying the stenosis level and the inlet velocity pulse frequency. The laminar flow is modeled solving the Navier-Stokes and continuity equations using an axis-symmetric coordinate system. The finite volume method is employed to perform the domain discretization and a coupled formulation is used to solve velocity and pressure fields. A language-C subroutine is developed to impose the inlet pulsatile velocity at the artery that are compiled inside the Fluent software as UDFs (User Defined Functions). To simulate the Casson viscosity model, an UDF is also created while for Newtonian model it is assumed a constant viscosity value. Three different Womersley number are considered: low (Wo = 4), moderate (Wo = 8) and high (Wo = 12), that induces period decrease and fast acceleration and deceleration as the Womersley number value increases. Hence, the artery stenosis level is changed (25%, 50% e 75%) to verify the Newtonian and Casson models behavior. Results are obtained for (i) stream function inside the artery domain, (ii) axial velocity contours/profiles and (iii) wall shear stress distribution. It is observed that Newtonian and Casson viscosity models results approximate only at high Womersley number (Wo = 12) and more intense stenosis level (75%).

Keywords: stenosed artery, hemodynamic, blood flow, Casson model, Womersley number.

1. INTRODUCTION

Blood flow is responsible for nutrient and waste transport within the closed-loop, cardiovascular network. Typically flow is laminar in healthy arteries, but the presence of abnormal flow conditions can promote the development of cardiovascular disease such as atherosclerosis and thrombus formation, Sinnott et al (2006). Arteries affected by atherosclerosis develop lesions which produce an accumulation of deposits on the arterial wall, ultimately affecting the flow pattern of the blood, Huang et al (1995).

It is also well known that the flow of blood depends on the pumping action of the heart which gives blood flow its pulsatile nature, Prakash and Ogulu (2007). Furthermore, there is also no doubt that under high velocity gradients the blood must be treated as a non-Newtonian fluid, and the dependence of viscosity with shear rate must be determined, Zamir (2000). In yet smaller vessels, a knowledge of the non- Newtonian blood rheology becomes essential to a correct understanding of its flow properties, Moyers-Gonzalez et al (2008). At this context, CFD simulations can be used to obtain detailed blood flow information, including wall shear stress, pressure drops, stagnation and recirculation regions, particle residence times, and turbulence, (Cebral et al, 2002).

Numerical simulation has been undertaken to attain a better understanding of functional, diagnostic and therapeutic aspects of the blood flow. Different viscosity models have been used to reproduce the non-Newtonian blood flow behavior. Shibeshi et al (2005) compared the most popular non-Newtonian models (power law, Casson and Carreau) to study the hemodynamics quantities in a T-junction geometry. Authors investigated the impact of the viscosity models on velocity profiles, wall shear stress and vortex length.

Sankar and Lee (2009) employed the Herschel–Bulkley model to study the pulsatile blood flow through mild stenosed artery. Their results showed that the velocity and the wall shear stress increase considerably with the increase in the amplitude of the pressure drop due to stenosis effect.

Other researchers have used Casson fluid model for mathematical modeling of blood flow through narrow and/or constricted arteries. Siddiqui et al (2009) investigated the pulsatility on flow through a stenosed artery using the Casson model to take account the non-Newtonian effects. Authors showed that the mean resistance to flow is greater in pulsatile flow when compared with steady flow conditions, whereas the mean value of the wall shear for pulsatile blood flow is equal to steady wall shear stress.

Sankar et al (2010) developed a theoretical model to study the pulsatile blood flow through mild stenosed narrow arteries by treating the blood in the core region as a Casson fluid and the plasma in the peripheral layer as a Newtonian fluid. They showed that the pressure drop, plug core radius, wall shear stress and resistance to flow increase as the yield stress or stenosis size increases while all other parameters were held constant.

In the work of Ponalagusamyn and Selvi (2011), the blood flow through an arterial stenosis was analyzed. The blood flow core region is assumed to be a Casson fluid and the peripheral layer of plasma as a Newtonian fluid. Authors obtained new analytic expressions for the thickness of the peripheral layer, slip velocity and core viscosity have been

obtained in terms of measurable quantities (flow rate, centerline velocity, pressure gradient, plasma viscosity and yield stress).

The present work intends to study the pulsatile blood flow on a stenosed artery. Three Womersley numbers are simulated employing the Casson viscosity model to take account the non-Newtonian blood flow features.

2. MATHEMATICAL MODELING

Figure 1 shows a schematic diagram model of a stenosed artery using an axisymmetric coordinate system, as studied by Pincombe and Mazumdar (1994). Blood flow is assumed to be laminar, incompressible and with constant properties. In this study, the artery wall elastic behavior is neglected.
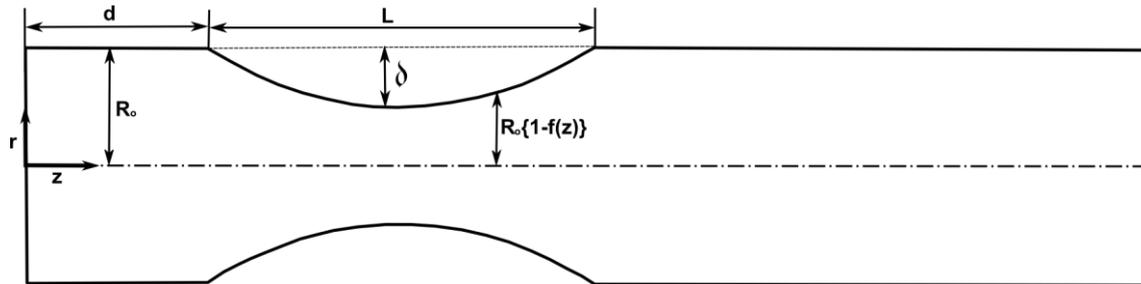

Figure 1. Schematic diagram of a stenosed artery.

Where:
r = radial coordinate
z = axial coordinate
R_0 = non-constricted artery radius
L = stenosed segment length
d = distance from the start of the arterial segment to the start of the stenosis
δ = stenosis depth

The constricted region (see Figure 1) of the artery domain is obtained using the following expressions:

$$\frac{R(z)}{R_o} = \begin{cases} 1 - f(z) & \text{for } d \leq z \leq d + L \\ 1 & \text{otherwise} \end{cases} \tag{1}$$

In which R is the artery radius throughout the constricted region and f(z) is given by:

$$f(z) = A[\, L^{n-1}(z-d) - (z-d)^n \,]\,, \text{ with } n = 2 \text{ and } A = \frac{\delta}{R_o L^n} \frac{n^{\frac{n}{n-1}}}{n-1}$$

The total tube lenght Z is equal to $6\,R_o$ and $L = 10$ mm.

It is well know that blood behaves as a non-Newtonian fluid under certain flow conditions, (Tu and Devile, 1996). Two characteristic features emerge from experimental data: (i) the presence of a yield stress and (ii) the dependence of the viscosity with respect to shear rate. To take these effects into account, the governing equations (continuity and momentum) are stated as:

$$\nabla \cdot \vec{v} = 0 \tag{2}$$

$$\rho \left[\frac{\partial \vec{v}}{\partial t} + (\vec{v} \cdot \nabla) \vec{v} \right] = -\nabla p + \nabla \cdot \tau \tag{3}$$

Where:
ρ = blood density; $\vec{v}$ = velocity vector; p = pressure field; t = time; $\nabla(\ )$ = gradient operator; $\nabla.(\ )$ = divergent operator,

τ = stress tensor expressed by:

$$\tau = \eta\,\gamma = \eta\left[\nabla\vec{v} + (\nabla\vec{v})^{tr}\right] \tag{4}$$

In Eq. 4 the superscript "tr" indicates the transpose; η is apparent viscosity of blood and γ is the shear rate. When the fluid is Newtonian, the stress tensor is proportional to the shear rate, and the constant of proportionality is called dynamic viscosity (μ). For Non-Newtonian fluids, the viscosity is called apparent viscosity (η) that, herein, is expressed according to the chosen model (see e.g. Casson model, expressed by Eq.5).

3. CASSON BLOOD VISCOSITY MODEL AND BOUNDARY CONDITIONS

Diverse forms of constitutive equations have represented the shear-thinning behavior of blood flow. The most common constitutive equations characterizing this rheological pattern are divided into two categories namely Newtonian and non-Newtonian models. Blood behaves as Newtonian fluids for shear rate above 200 s^{-1} (Berger and Jou, 2000), as shown in Figure 2 (see Newtonian model with a single value viscosity equal to 0.0035 Pa.s). The power law model adjust satisfactory to experimental results at low shear rate values. It is also observed that Casson viscosity model presents a better agreement in comparison with experimental data provided by Fournier (2007) for the entire shear rate plotted interval.
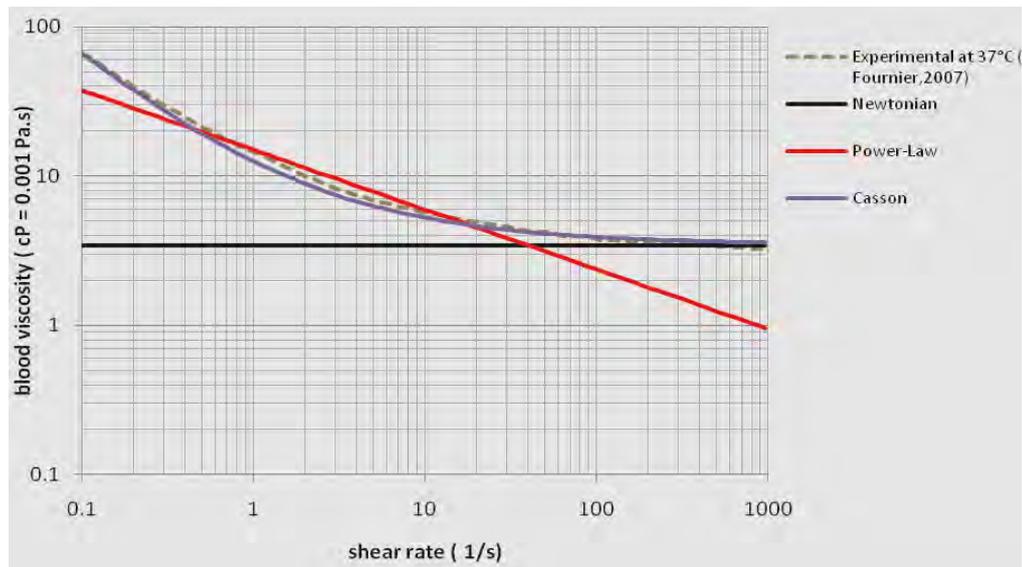

Figure 2. Blood viscosity models and experimental results**.**

The Casson viscosity model takes into account that blood at rest requires a minimum yield stress (τ_0) to start flowing. This blood behavior is modeled by the following equation:

$$\eta = \frac{\tau_0}{\gamma} + \frac{\sqrt{C\tau_0}}{\gamma} + C \tag{5}$$

where η is the viscosity of blood, γ is the shear stress, τ_0 yield stress and C is the Casson rheological constant. The values of τ_0 and C depends on hematocrit H. Hematocrit is a percentage of whole blood occupied by cellular elements.

The non-linear partial differential equation system represented by Eq. 2 to 4 requires appropriate boundary conditions. At the present study, no-slip boundary conditions were imposed at rigid walls and a null value to the pressure was specified at the artery outlet. At the inlet, a pulse axial velocity *v(t)* with time-varying function is imposed, as shown in Figure 3.

$v(t) = 3 + 3sin\ (2\pi t/T)$ (6)
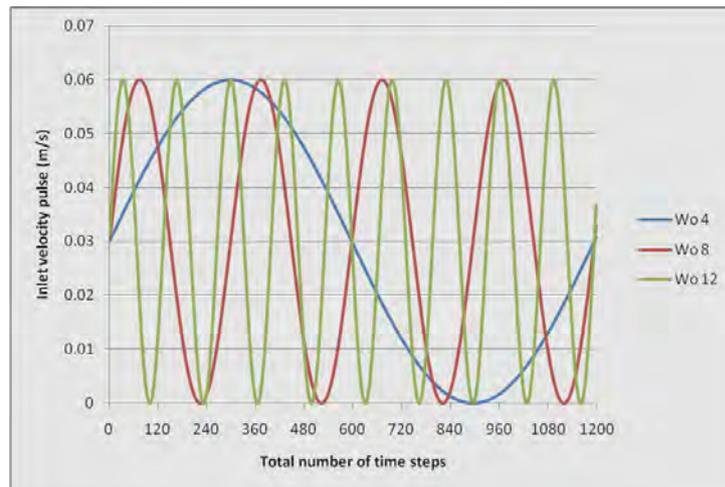
Where: T = period and t = time.

Figure 3. Inlet velocity pulse for different Womersley numbers.

For pulsatile flow, two dimensionless parameters are commonly used to characterize the flow conditions: (i) the Reynolds number $R_e = \dfrac{\rho \bar{v}(2R)}{\mu}$, where ρ is density of the fluid, $\bar{v}$ is the characteristic velocity determined as the time-averaged mean velocity and μ is dynamic viscosity and (ii) the Womersley number $\alpha = R\left(\dfrac{\varpi}{v}\right)^{0.5}$ with $\varpi = 2\pi/T$ is the frequency of the cyclic variation, R is the tube radius, and v is the kinematic viscosity. While the Reynolds number is a comparison of the inertial to viscous forces, the Womersley number can be interpreted as the ratio of the unsteady to viscous forces. Usually, high Womersley number (Wo > 10) correspond to conditions of blood flow with intense acceleration and deceleration.

4. SOLUTION METHODOLOGY

The governing equations system (Eq. 2 to Eq. 4) was discretized by the finite volume method employing a CFD package. The pressure-velocity fields are coupled using the SIMPLE algorithm and the convective terms are treated by second order discretization. The Casson viscosity model was numerically implemented as a UDF C-language subroutine interpreted by the Fluent code. These main parameters are listed in Tab.1. A computational mesh with quad elements was generated, as can be seen in Fig. (4). When the numerical residual reaches 10^{-5}, the solution is considered as converged.

Table 1. Blood viscosity models input parameters used in the simulations.

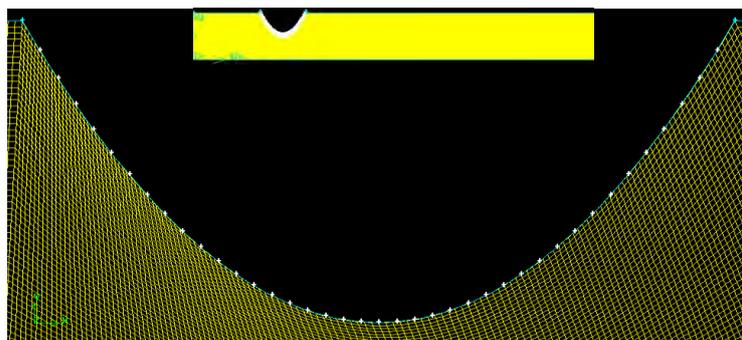| Blood viscosity	Input parameters
Newtonian Model	$\rho = 1050\ kg/m^3$ and $\mu = 0.00345\ Pa.s$
Casson Model	$\tau_0 = 0.005\ N$ and $C = 0.0035\ Pa.s$

Figure 4. Mesh generated for the stenosed artery with a "zoom" region.

5. RESULTS AND DISCUSSION

Numerical simulations were conducted by testing three artery obstruction levels. Figure 5 shows the geometry and final mesh for 25%, 50% and 75% stenosis conditions. The stenosed segment length (*L* in Figure 1) is constant and the stenosis depth *(δ)* is equal to 2.5 mm, 5.0 mm and 7.5 mm, respectively.
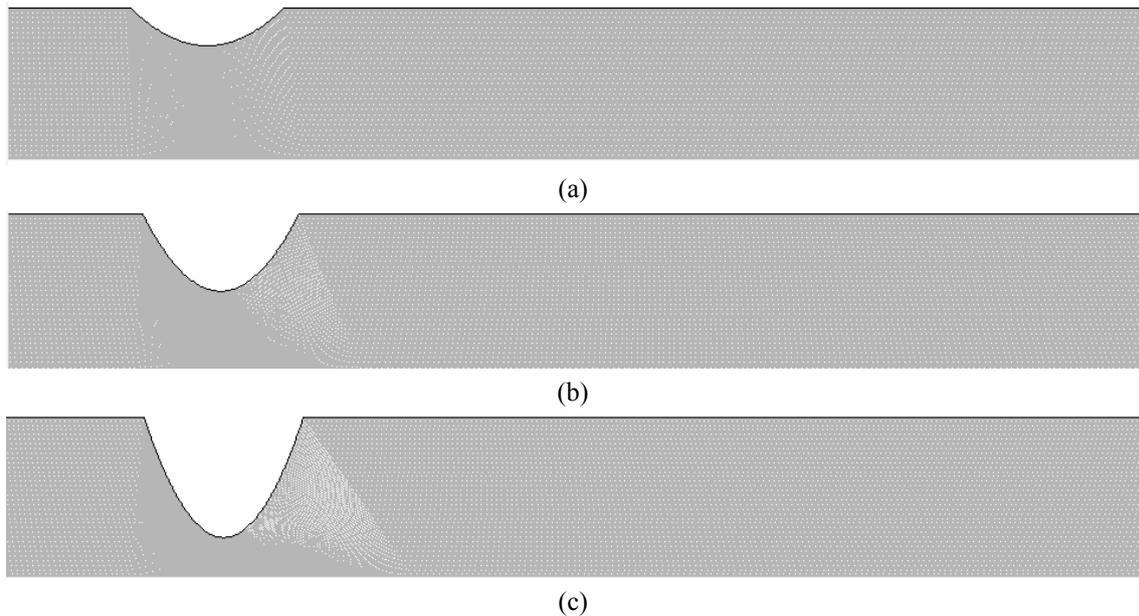

(a)

(b)

(c)

Figure 5. Geometry for the stenosed artery with: (a) 25% obstruction; (b) 50% obstruction and (c) 75% obstruction

For 50% obstruction, the results for the shear stress along the artery upper wall are shown Figure 6 for Newtonian and Casson viscosity models as a function of the Womersley number. It is observed a strong increase in the shear stress close to the stenosis region ($0.1 < z/L < 0.2$) due to high velocity gradients caused by flow constriction in this area. it is also noted that the Newtonian approach (Fig. 6a) does not well capture the increase in the shear stress as the Wo decreases. The Casson model (Fig. 6b) exhibits a maximum value of approximately 4 Pa for the shear stress when Wo = 4, while the Newtonian model value is about 2 Pa. Similar behavior has been obtained for 25% and 75% stenosis cases.
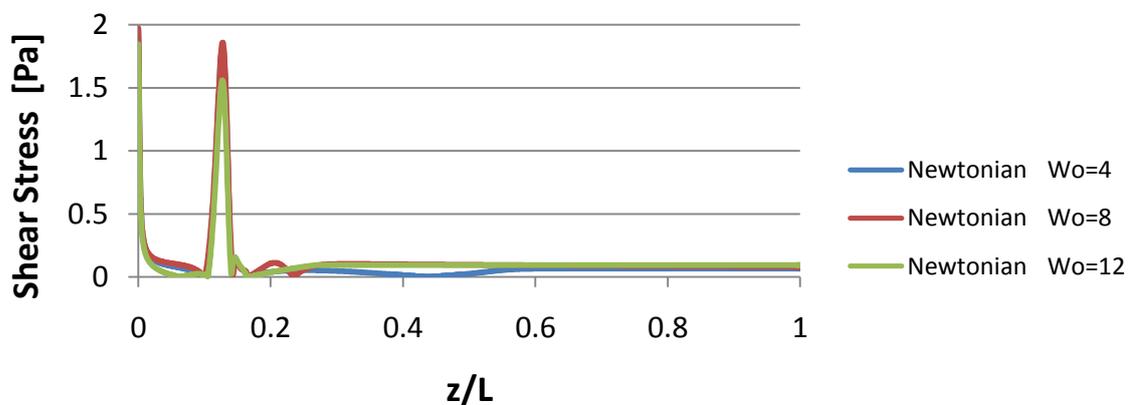

(a)
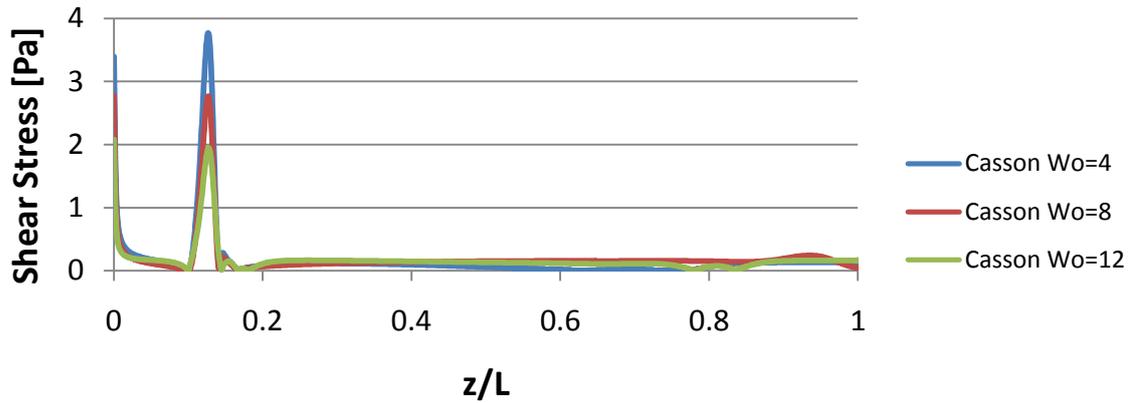
(b)

Figure 6. Shear stress along the artery upper wall for 50% obstruction: (a) Newtonian model and (b) Casson model.

As the Casson model better reproduces the blood flow pattern (see also Figure 2), all hereinafter presented results were obtained employing this constitutive viscosity equation. Figure 8 shows stream-function distribution inside the stenosed artery for 50% stenosis levels with Wo = 4, 8 and 12. These frames corresponds to instant of peak in the inlet pulsatile velocity with $v(t)$ = 0.06 m/s (Figure 3) and the time step number varies according to each simulated Womersley number. It is observed that for Wo = 4 (Figure 7a), the recirculation zone is close to the stenosis area. Then, the stream-function magnitude increases as the Wo number elevates, but the recirculation zone migrates downstream the stenosis region. As the Womersley number increases, the blood flow is subjected to rapid acceleration and deceleration, occurring a displacement of the region with maximum stream-function values downstream of the constricted area. Consequently, the velocity gradients around the stenosis region are reduced, occurring a decrease in the shear stress peak as observed in the Figure 6b.
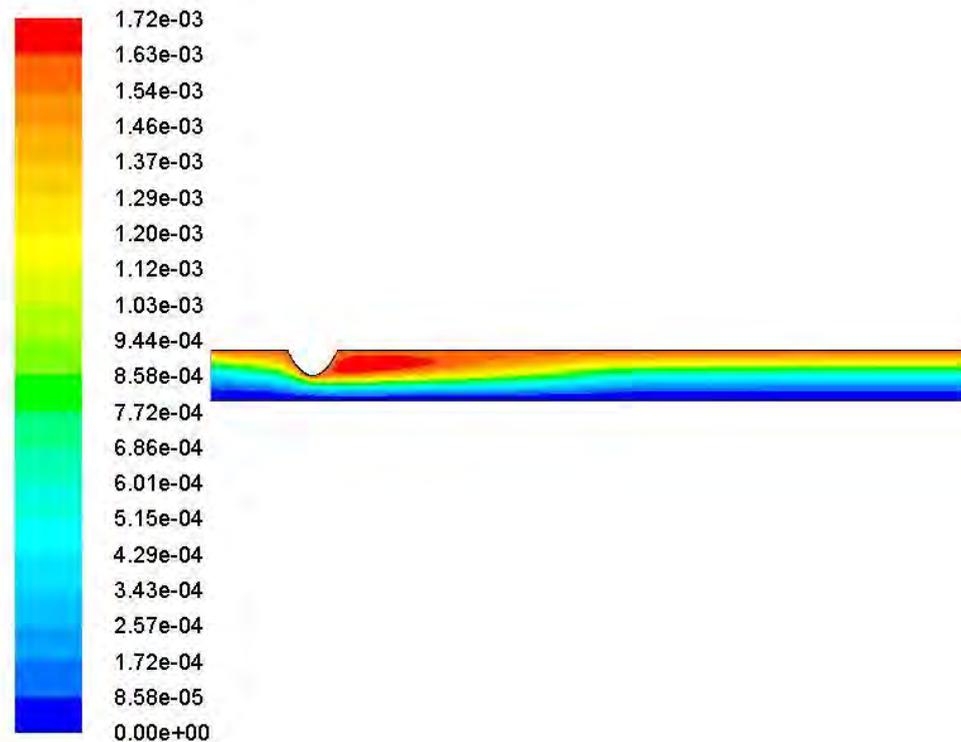

(a)
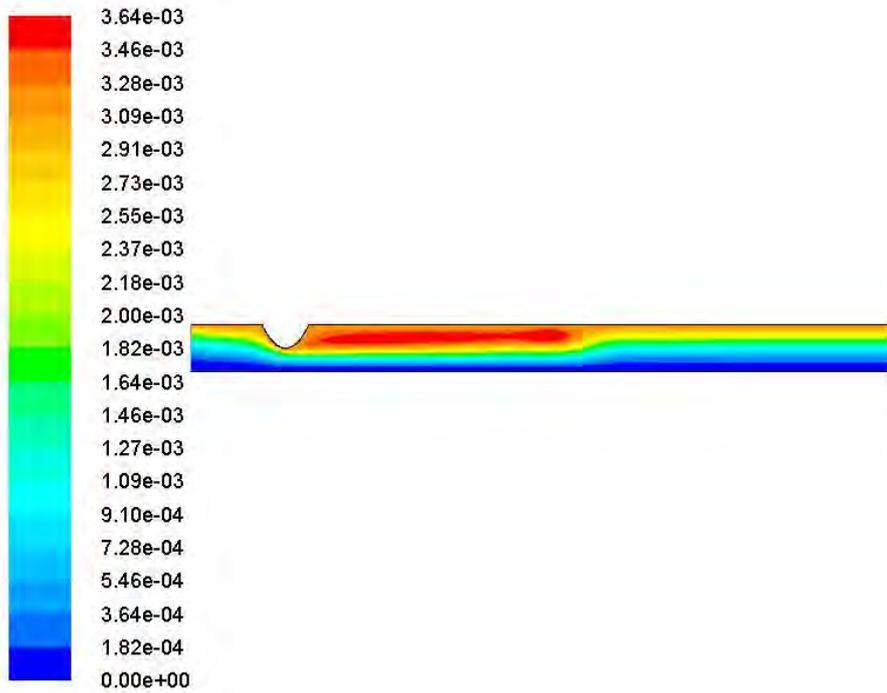
(b)
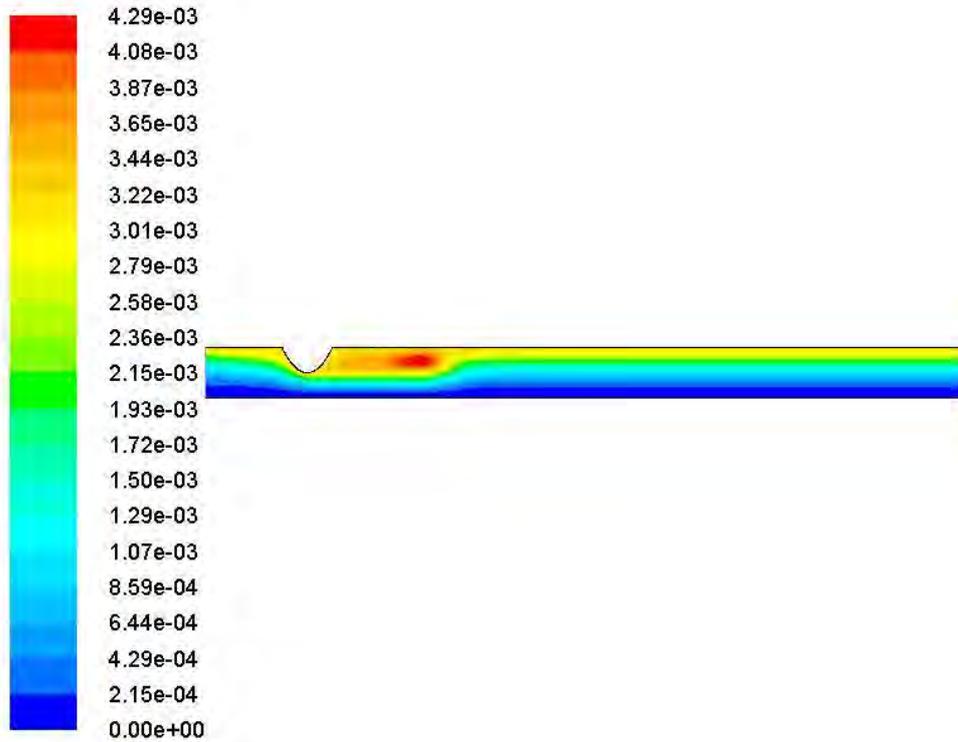
(c)

Figure 7. Stream function pattern inside stenosed artery for 50% stenosis: (a) Wo = 4; (b) Wo = 8; (c) Wo = 12 (Casson model).

Figure 8 shows stream-function distribution inside the stenosed artery for Wo = 12 with 25%, 50% , and 75% stenosis levels. When the stenosis level is smooth (25% obstruction , Figure 8a), the blood flow is little disturbed (maximum values of = $3.2 \cdot 10^{-3}$ kg/s) and the recirculation region is practically inexpressive. However, for 50% obstruction (Figure 8b), a recirculation zone appears downstream the stenosis area occurring an increase in the flow intensity (maximum of $4.3 \cdot 10^{-3}$ kg/s).
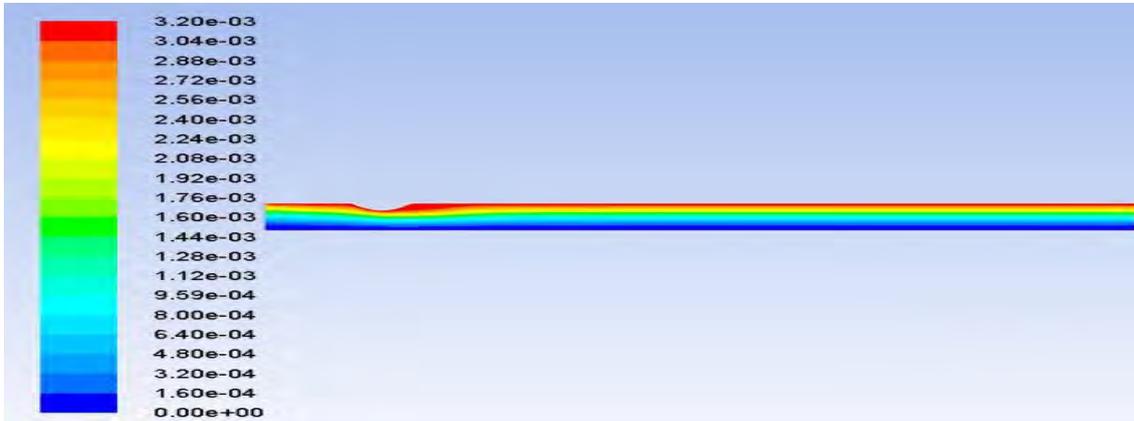
(a)
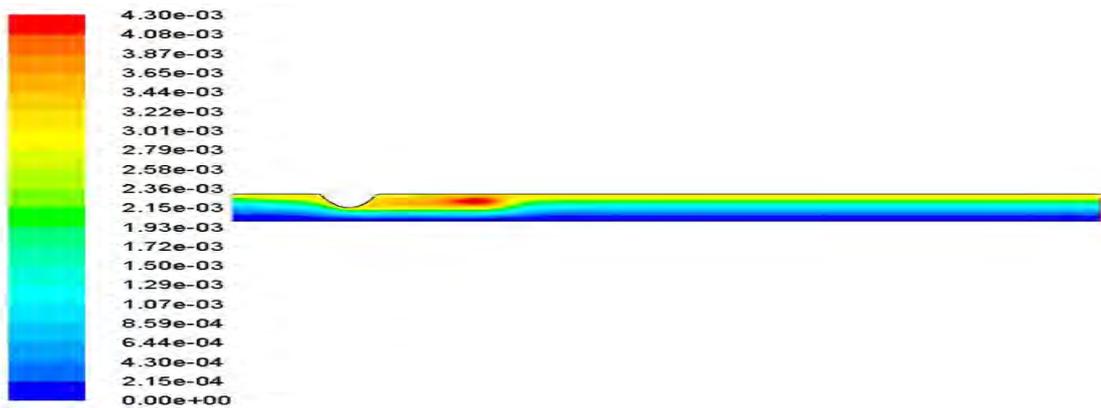
(b)
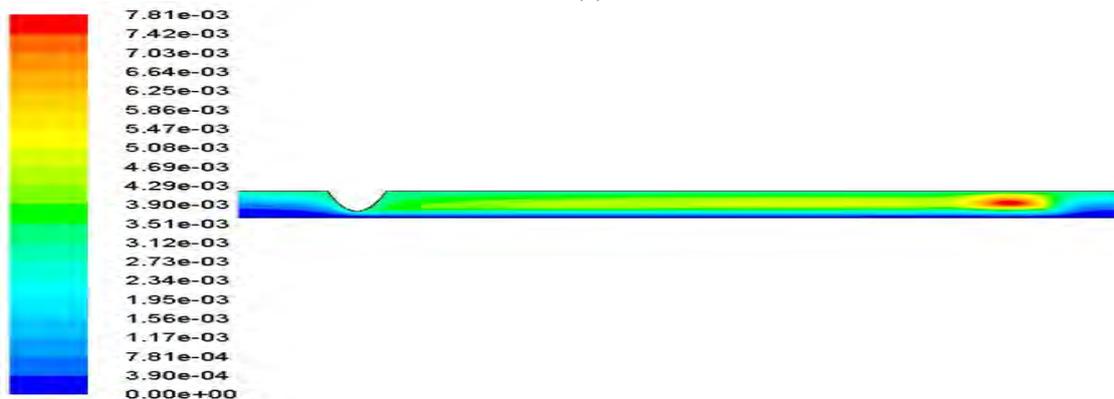
(c)

Figure 8. Stream function pattern inside stenosed artery for Wo = 12: (a) 25% stenosis; (b) 50% stenosis; (c) 75% stenosis (Casson model).

Figure 8c (75% stenosis) shows that the blood flow is strongly throttled close to the stenosis region and the recirculation area migrates far from the constricted position. It is important to remember that these conditions have been established under transient regime. Therefore, these frames corresponds to the beginning of the acceleration phase imposed by the inlet pulsatile flow with ($v(t)$ = 0.045m/s (see Figure 3).

6. CONCLUDING REMARKS

Pulsatile blood flow was numerically simulated comparing Newtonian and Casson viscosity model approaches. Results showed that the Newtonian model does not well capture shear stress peaks occurred at the artery upper wall due to stenosis effect. Thus, the Casson model was employed to study the Womersley number effect varying the stenosis level. It was observed that for high Wo numbers, the blood flow intensity also increases and the recirculation zone caused by the stenosis was displaced downstream the constriction region. This behavior was also intensified as the artery obstruction level increased (from 25% to 75%).

7. REFERENCES

Berger S. and Jou L., 2000, "Flows in Stenotic Vessels". *Annual Review of Fluid Mechanics*, 32, 347–382 pp.

Cebral, J.R., Yim P.J., Löhner, R., Soto, O. and Choyke, P.L., 2002, Blood Flow Modeling in Carotid Arteries with Computational Fluid Dynamics and MR Imaging, *Academic Radiology*, 9, 1286-1299 pp.

Fournier, R. L., 2007, "Basic Transport Phenomena in Biomedical Engineering", Ed.Taylor & Francis, New york, USA, 450 p.

Huang, H., Modi, V.J. and Seymour, B.R., 1995, Fluid Mechanics of Stenosed Arteries, *Int. J. Engng Sci.*, 33 (6), 815-828 pp.

Moyers-Gonzalez, M. A., Owensa R. G. and Fang J., 2008, "A non-homogeneous constitutive model for human blood Part III. Oscillatory flow", *J. Non-Newtonian Fluid Mech*., 155, 161-17 pp.

Pincombe, B. and Mazumdar, J., 1994, "A Mathematical Study of Blood Flow through Viscoelastic Walled Stenosed Arteries, Aust. Phys. Engng. Sci. Med., 18, 81-88 pp.

Ponalagusamyn, R. and Selvi, R.T., 2011, "A study on two-layered model (Casson–Newtonian) for blood flow through an arterial stenosis: axially variable slip velocity at the wall", Journal of the Franklin Institute, 348, 2308–232 pp.

Prakash, J. and Ogulu, A., 2007, "A study of pulsatile blood flow modeled as a power law fluid in a constricted tube", *International Communications in Heat and Mass Transfer*, 34, 762-768 pp.

Rohlf, K. and Tenti, G., 2001, "The role of the Womersley number in pulsatile blood flow: a theoretical study of the Casson model", Journal of Biomechanics, 34 (2001) 141-148 pp.

Sankar, D.S. and Lee, U., 2009, "Mathematical modeling of pulsatile flow of non-Newtonian fluid in stenosed arteries, Commun. Nonlinear Sci. Numerical Simulation, 14, 2971–2981 pp.

Sankar, D.S. and Lee, U., 2010, "Two-fluid Casson model for pulsatile blood flow through stenosed arteries: A theoretical model", Commun. Nonlinear Sci. Numerical Simulation, 15, 2086–2097 pp.

Shibeshi, S.S. and Collins, W.E., 2005, The Rheology of Blood Flow in a Branched Arterial System, *Appl Rheol*., 15(6), 398–405 pp.

Siddiqui, S.U., Verma, N.K., Mishra, S. and Gupta, R.S., 2009, "Mathematical modelling of pulsatile flow of Casson's fluid in arterial stenosis", *Applied Mathematics and Computation*, 210, 1–10 pp.

Sinnott, M., Cleary, P. W. and Prakash, M., 2006, An Investigation of Pulsatile Blood Flow in a Bifurcation Artery Using a Grid-Free Method, Fifth International Conference on CFD in the Process Industries, CSIRO, Melbourne, Australia.

Tu, C., Deville, M., Dheur, L., and Vnderschuren, L., 1992, "Finite-element simulation of pulsatile flow through arterial stenosis". *J. Biomechanics*, 25, 1141-1152 pp.

Zamir, M., 2000. "The physics of pulsatile flow". Ed. Springer-Verlag, New York,Inc ,220 p.

8. RESPONSIBILITY NOTICE

The authors are the only responsible for the printed material included in this paper.